



ORIGINAL ARTICLE

Effect of weighting materials on carbonation of oil well cement-based composites under high temperature and CO₂-rich environment



Zhongtao Wu^{a,b,c}, Jianjian Song^{a,b,c,d,*}, Mingbiao Xu^{a,b,c,d}, Weihong Liu^{a,b,c,d},
Rongyao Chen^{b,c}, Lei Pu^{b,c}, Shanshan Zhou^{b,c}

^a Cooperative Innovation Center of Unconventional Oil and Gas (Ministry of Education & Hubei Province), Yangtze University, Wuhan 430100, PR China

^b School of Petroleum Engineering, Yangtze University, Wuhan 430100, PR China

^c Hubei Key Laboratory of Oil and Gas Drilling and Production Engineering (Yangtze University), Wuhan 430100, PR China

^d National Engineering Research Center for Oil and Gas Drilling and Completion Technology (Yangtze University), Wuhan 430100, PR China

Received 30 October 2022; accepted 9 February 2023

Available online 15 February 2023

KEYWORDS

Oil well cement-based composites;
Carbonation;
Weighting materials;
High temperature;
Carbon dioxide

Abstract As an indispensable part of cement slurry for high temperature and high pressure oil and gas wells, weighting materials have a significant impact on the carbon dioxide corrosion of oil well cement-based composites. This paper studied the carbonation process of cement with three weighting agents, and evaluated the compressive strength and carbonation depth of cement at 150 °C. XRD, SEM and MIP were used to study the carbonation mechanism of cement. When 21 days of carbonation, the carbonation depth growth rate of hausmannite cement was 0.21 mm/d, hematite cement was 0.24 mm/d, and barite cement was 0.31 mm/d. The compressive strength of cement decreased after carbonation, and the carbonation had a minor influence on the compressive strength of hausmannite cement and the most significant impact on barite cement. The carbonation product of oil well cement was mainly calcite. Unstable vaterite mainly existed in the barite cement sample, indicating that the barite cement sample was the most serious corrosion. In the carbonation zone, the number of pores smaller than 10 nm increased the most in the hausmannite cement sample. Pores with a diameter greater than 100 nm accounted for 1.9 % in the hausmannite cement,

* Corresponding author at: Cooperative Innovation Center of Unconventional Oil and Gas (Ministry of Education & Hubei Province), Yangtze University, Wuhan 430100, PR China.

E-mail address: songjian629@yangtzeu.edu.cn (J. Song).

Peer review under responsibility of King Saud University.



3.0 % in hematite cement, and 4.8 % in barite cement. The result shows that hausmannite is the most conducive to the corrosion resistance of oil well cement.

© 2023 The Author(s). Published by Elsevier B.V. on behalf of King Saud University. This is an open access article under the CC BY-NC-ND license (<http://creativecommons.org/licenses/by-nc-nd/4.0/>).

1. Introduction

Cementing operation plays a vital role in the development of oil and gas wells. Cement slurry is injected into the annulus between the casing and the wellbore in cementing operations. The cement slurry sets to form a cement sheath. The cement sheath supports the casing, seals the leakage zone, and prevents cross-flow of fluids (oil, gas, and water) between the formations. So the integrity of cement sheath is critical to ensure the production safety of oil and gas wells. Chemical reactions are a common factor affecting the integrity of the cement sheath. Because Portland cement is commonly used in well cement, the hydration products of the cement are rich in alkaline substances, so they are vulnerable to acid fluid erosion (Kiran et al., 2017). Common acidic fluids in the formation are CO₂ and H₂S, of which CO₂ is the main factor leading to cement sheath corrosion (Krilov et al., 2000). Although CO₂ gas is not corrosive, it reacts with water to form carbonic acid, which may lead to the carbonation and dissolution process of cementitious phases, followed by the leaching of carbonate and increasing porosity and permeability, finally creating pathways through a casing surface. Upon leakage of CO₂ aqueous solution into the casing surface, corrosion processes, including localized and pitting, can occur. This can dramatically reduce the life of oil and gas wells (Hoa et al., 2021).

There are two primary sources of CO₂ near-wellbore: artificial injection and inorganic origin. Artificial injection mainly occurs in carbon capture and storage (CCS) wells, CO₂ is injected into deep saline, coal beds, and depleted reservoirs to store it for long-term storage (Bachu, 2000; Lesti et al., 2013; Vishal et al., 2021). In addition, in terms of enhanced oil recovery, CO₂ flooding technology (Lu et al., 2021), CO₂ fracturing technology (Nianyin et al., 2021), and CO₂ replacement technology (Wang et al., 2021) have broad application prospects due to the unique physical and chemical characteristics of CO₂ fluid. Inorganic CO₂ in the strata is mainly derived from the degassing of the mantle and volcanic rock, which is migrated and accumulated to form CO₂ gas reservoirs (Guang et al., 2011), which will be

mined together when mixed with oil and gas. When CO₂ is abundant near the wellbore, the integrity of the cement sheath is severely tested. The design difficulty of the cement slurry is how to reduce the corrosion of CO₂ on oil well cement-based composites.

Researchers have done many studies on cement slurry in the environment where carbon dioxide exists, and some scholars have written relevant reviews (Bagheri et al., 2018; Teodoriu and Bello, 2020). Table 1 shows the experimental conditions of laboratory experiments of oil well cement in a carbonic acid environment conducted by some scholars in recent years. The carbonation experiment of oil well cement under high temperature is relatively few, and the carbonation experiment of cement under high temperature and high pressure is relatively few involving the influence of weighting materials on the carbonation of cement. However, the carbonation of oil well cement in high-temperature and high-pressure environments cannot be ignored. CO₂-rich high temperature reservoirs are found in the Krishna Godavari basin on the east coast of India (Shah et al., 2012), Persian Gulf Basin (Abed et al., 2010), Oman salt basin in South Sudan (Fakhr Eldin et al., 2009), Northern Kuwait (Abdel-Basset et al., 2021), Sichuan Basin (Wei et al., 2015), and Yinggehai Basin in the South China Sea (Jihai and Huang, b., 2019). Taking the South China Sea as an example, its maximum pressure coefficient is 2.38, seabed temperature is 480°C, and CO₂ concentration is 50 % (Shujie et al., 2020). Due to the different hydration mechanisms of cement at different temperatures, the influence on carbonation is also different (Omosebi et al., 2015). At the same time, high temperature will promote the carbonation rate of oil well cement-based composites (Drouet et al., 2019), and CO₂ solubility increases with the increase of pressure (Allen et al., 2005). These factors make the carbonation of cement under high temperature and high pressure more complicated.

Applying a high-density cement slurry to balance formation pressure is often necessary for high temperature and high pressure oil and gas wells. Generally, increase the slurry density by adding weighting agents. Weighting agents used in oil well cement are usually inert

Table 1 Test conditions of cement carbonation experiment.

| Data sources | Test conditions | |
|---|--------------------------|------------------------|
| | Maximum temperature (°C) | Maximum pressure (MPa) |
| Mei et al. (2021) (Mei et al., 2022) | 62 | 17 |
| Ponzi et al. (2021) (Ponzi et al., 2021) | 65 | 15 |
| Tiong et al. (2020) (Tiong et al. 2020) | 70 | 24 |
| (Costa et al. (2021) Costa et al., 2021) | 70 | 13 |
| Engelke et al. (2017) (Engelke et al., 2017) | 74 | 24 |
| Contreras (2021) (Contreras and Santra, 2021) | 82 | 20 |
| Yang et al. (2016) (Yang et al., 2016) | 85 | 20 |
| Ledesma et al. (2019) (Ledesma et al., 2020) | 90 | 15 |
| Batista et al. (2020) (Batista et al., 2021) | 90 | 15 |
| Xu et al. (2019) (Xu et al., 2019) | 90 | 20 |
| Sedić et al. (2020) (Sedić et al., 2020) | 100 | 7 |
| Xin et al. (2020) (Xin et al., 2020) | 100 | 5 |
| Jani et al. (2021) (Jani and Imqam, 2021) | 110 | 10 |
| Bjørge et al. (2019) (Bjørge et al., 2019) | 120 | 28 |
| Elkatatny (2020) (Elkatatny, 2021) | 130 | 10 |
| Ridha et al. (2021) (Ridha et al., 2021) | 130 | 24 |
| Mahmoud et al. (2020) (Mahmoud and Elkatatny, 2020) | 130 | 10 |
| Srivastava et al. (2019) (Srivastava et al., 2019) | 221 | 63 |
| Omosebi et al. (2015) (Omosebi et al., 2015) | 221 | 62 |

materials, which significantly impact the rheology, fluid loss, and compressive strength of the cement slurry. As a result, the design of high-density cement slurry is more complex than that of conventional cement slurry. In terms of the selection of weighting agent, the weighting materials used in oil well cement-based composites to improve the density of cement slurry mainly include barite, hausmannite and hematite. Under higher temperatures such as geothermal steam injection and ultra-deep Wells, hematite, hausmannite, and ilmenite are no longer inert in cement slurries with temperatures above 302 °C, while barite is still inert under such conditions (Ramazanov et al., 2021; Caritey and Brady, 2013). To obtain a higher filling amount, some scholars selected spherical particle Micromax weighting agent, reduced iron, and hematite to combine to improve the rheological properties of cement slurry and achieve a tighter stacking effect, and further obtained ultra-high-density cement slurry with a density of 2.7 ~ 3.0 g/cm³ (Shiming et al., 2013). As weighting material is an essential component of high temperature resistant and high density cement slurry, for oil and gas wells containing carbon dioxide acid gas, it is necessary to study the effect of weighting agent on carbon dioxide corrosion of oil well cement-based composites.

There are few studies on the application of cement weighting agents in oil wells under the condition of high temperature and rich CO₂. Considering the different fillers under the environment of high temperature of oil well cement's carbonation resistance ability may produce a different effect, so this paper analyzes three kinds of commonly used fillers: hausmannite (Mn₃O₄), hematite (Fe₂O₃), and barite (BaSO₄), for evaluation of slurry for adding different weighting agents under the environment of high temperature and high CO₂ concentration carbonation resistance, and the influence mechanism of cement carbonation of weighting materials.

2. Materials and methods

2.1. Materials

Class-G oil well cement was used from Sichuan Jiahua Special Cement Factory (Chengdu, China). Table 2 shows the chemical composition of cement. 35 wt% silica sand was added to avoid the compressive strength decline of oil well cement-based composites at high temperatures. The fluid loss additive, defoamer, and dispersant used in the experiment came from Jingzhou Jiahua Technology Co., Ltd. Dispersant is used to ensure the fluidity of the cement slurry when too much weight-

ing agent is added. The microscopic morphology of hausmannite (Mn₃O₄), hematite (Fe₂O₃), and barite (BaSO₄) are shown in Fig. 1. Table 3 shows the composition of different cement slurries.

2.2. Methods

2.2.1. Sample preparation

The solid material was weighed before mixing with the liquid and mixed evenly. The liquid admixture was first added to water and was stirred evenly at a speed of 3800 ~ 4200r/min, and then the solid material was added slowly in the 30 s. After adding the ingredients, put the lid on the mixing cup and continue to stir for 35 s at 11,000–12,000r/min. Due to the large volume of cubic cement sample with an API standard side length of 2in, the carbonation reaction is not obvious in a relatively short time, cylindrical cement samples with a small volume can be selected for the carbonation experiment (Bruckdorfer, 1986). The mixed cement slurry was poured into a cylindrical metal mold with a bottom diameter of 25 mm and a height of 25 mm as shown in Fig. 2 and manually stirred for defoaming. Then put the slurry mold into a curing kettle for three days. The temperature of the curing kettle was set as 150 °C and the pressure as 21 MPa. The temperature and pressure rise rate was set as 0.63 °C/min and 0.09 MPa/min.

2.2.2. Carbon dioxide corrosion test of cement samples

Put the sample used for carbonation into the carbonation test reaction vessel, as shown in Fig. 3, and fill the carbonation instrument with 70 % CO₂ and 30 % N₂. The carbonation temperature was 150 °C, and the pressure in the reaction vessel was 30 MPa.

2.2.3. Compressive strength test

The cement sample was placed on the supporting block of the mechanical testing machine and ensured that the supporting block with a spherical base was balanced and could be tilted freely. The loading rate was set at 1.2kN/s to measure the unconfined compressive strength of the cement sample.

2.2.4. Carbonation depth

The circular corrosion profile was obtained by cutting the cylinder cement in the middle of the side. Because the carbonized zone was depleted of alkaline materials and the uncarbonized middle part is rich in alkaline materials, the carbonation part could be distinguished from the uncarbonized part by phenolphthalein reagent titration. The uncar-

Table 2 Chemical composition of Class-G cement.

| Chemical composition (wt%) | | | | | | |
|----------------------------|------------------|--------------------------------|--------------------------------|------|-----------------|--------|
| CaO | SiO ₂ | Fe ₂ O ₃ | Al ₂ O ₃ | MgO | SO ₃ | Others |
| 64.15 | 22.93 | 4.55 | 2.88 | 1.45 | 2.11 | 1.93 |

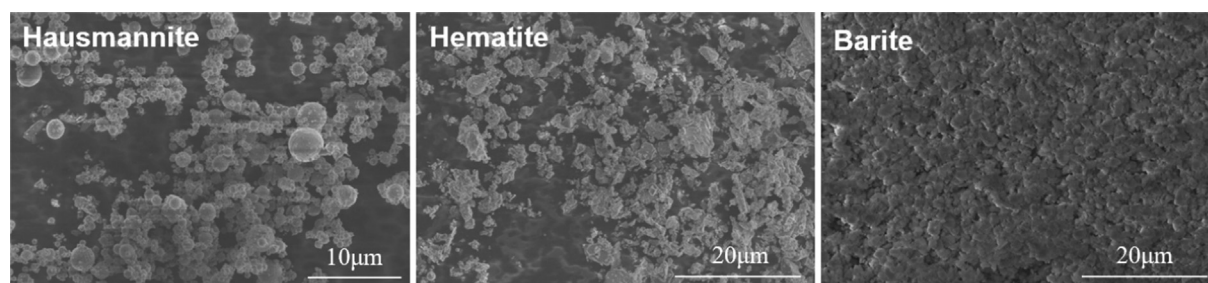
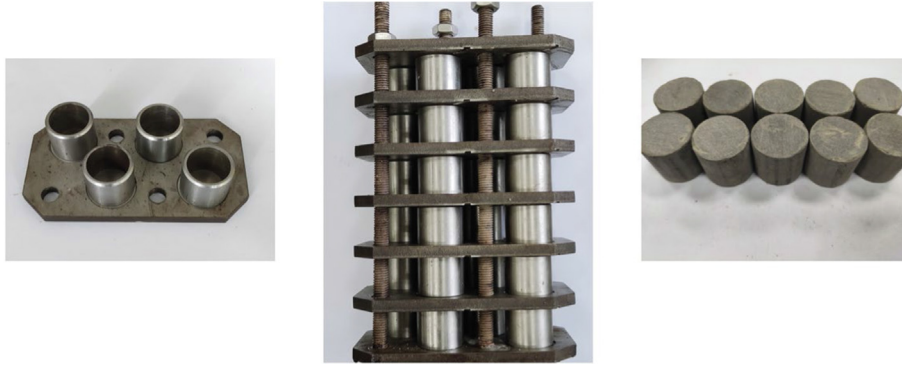


Fig. 1 SEM images of weighting agent.

Table 3 The composition of different cement slurries.

| Mixes(wt. %) | OPC | Silica powder | Fresh water | Filtrate reducer | Defoamer | Dispersant | Hausmannite | Hematite | Barite |
|--------------|-----|---------------|-------------|------------------|----------|------------|-------------|----------|--------|
| NWC | 100 | 35 | 44 | 5 | 1 | | | | |
| MC | 100 | 35 | 44 | 5 | 1 | | 50 | | |
| FC | 100 | 35 | 44 | 5 | 1 | | | 50 | |
| BC | 100 | 35 | 44 | 5 | 1 | | | | 50 |
| MC25 | 100 | 35 | 44 | 5 | 1 | 2.5 | 25 | | |
| MC50 | 100 | 35 | 44 | 5 | 1 | 2.5 | 50 | | |
| MC75 | 100 | 35 | 44 | 5 | 1 | 2.5 | 75 | | |

**Fig. 2** Diagram of metal mold and cylindrical cement samples.

bonized zone of cement was calculated by ImageJ image processing software. Eq. (1) is used to calculate the carbonation area of cement. By Eq. (2), Eq. (3), and Eq. (4), the average carbonation depth, the proportion of carbonation zone, and the carbonation rate of cement are calculated, respectively.

$$S_2 = \pi \left(\frac{D}{2} \right)^2 - S_1 \quad (1)$$

$$d = \left(\frac{D}{2} \right) - \sqrt{\frac{S_1}{\pi}} \quad (2)$$

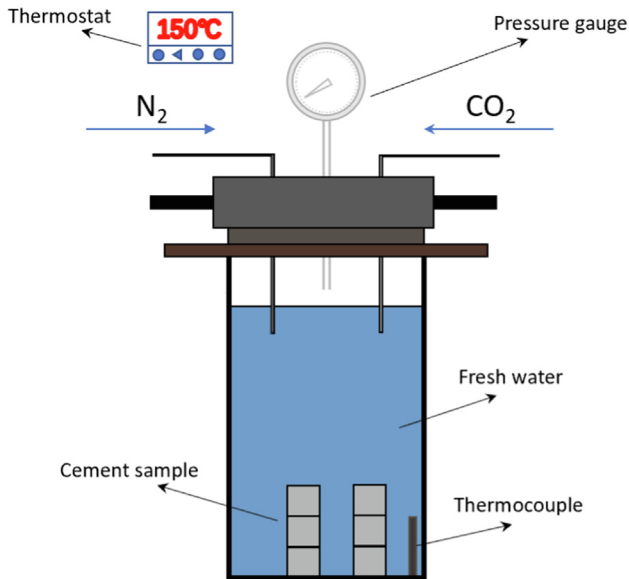
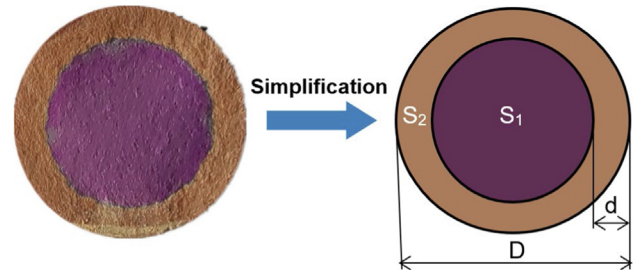
$$P = \frac{S_2}{S_2 + S_1} \times 100\% \quad (3)$$

$$v = \frac{d}{t} \quad (4)$$

As shown in Fig. 4, D is the diameter of the cement rock bottom; S_2 is the carbonation zone; S_1 is the zone of the uncarbonated zone; d is the average carbonation depth; P is the proportion of carbonized zone; v is the carbonation rate; t is carbonation time.

2.2.5. X-ray diffraction analysis

The Bruker D8-Advance X-ray diffractometer was used to analyze the phase composition of cement samples. After carbonation for 30 days, the carbonized zone and the uncarbonated zone of cement were sampled, ground into powder,

**Fig. 3** Carbonation test reaction vessel.**Fig. 4** Carbonation depth simplified diagram.

and dried in an oven of 60 °C for 24 h. The experiment was conducted with Cu-K α radiation, and the angle range was 5°~90°.

2.2.6. Scanning electron microscope test

The SU8010 scanning electron microscope was used to analyze the microstructure. The cement sample was dried after carbonation for 30 days. After drying, the sample surface was sprayed with gold to obtain better image quality.

2.2.7. Pore diameter distribution

The AutoporeII9220 mercury intrusion porosimetry from Micromeritics was used to measure the pore size distribution of cement-based materials. Small pieces of cement in carbonized and uncarbonized areas were selected. To avoid the residual moisture in tiny pores influencing the test results, samples were dried in 105 °C ovens for 24 h before the test.

3. Results and discussion

3.1. Effect of weighting agent on the properties of corroded cement paste

3.1.1. Effect of different weighting agents on carbonation depth

The carbonation degree of cement can be evaluated according to the carbonation depth, which is determined using phenolphthalein indicator. Carbonation depth is the most intuitive evi-

dence to measure the carbonation rate of oil well cement-based composites (Ponzi et al., 2021; Costa et al., 2021; Mi et al., 2021). Fig. 5 shows the cross-sections of cement carbonation for 3, 9, and 21 days. With the increase of carbonation time, the carbonation depth of cement samples gradually becomes more extensive. When the carbonation time reaches 21 days, the carbonation zone of different types of cement samples can be observed by visual significantly different. The uncarbonized area S1, the average carbonation depth d , and the proportion of carbonized zone P were calculated after 21 days of carbonation of cement, as shown in Table 4. Among them, the carbonation depth of cement with a weighting agent is less than that without weighting agents. Among the cement containing weighting agents, the carbonation depth of hausmannite cement is the lowest, followed by hematite cement, and barite cement carbonation depth is the largest. The carbonation depth of barite cement is 50.2 % larger than that of hausmannite cement and 31.3 % larger than that of hematite cement. The carbonation zone of barite cement accounted for 77.3 % of the whole cross-section zone, while the hausmannite cement was only 57.6 %.

Table 5 shows the carbonation rate of cement in different periods. It can be known that the carbonation rate of cement in the first three days is the largest, and the carbonation rate of cement in the later period is far less than the carbonation rate of the first three days. Pores with larger diameter play a dominant role in carbon dioxide diffusion. The faster carbonation reaction mainly occurred in the early carbonization

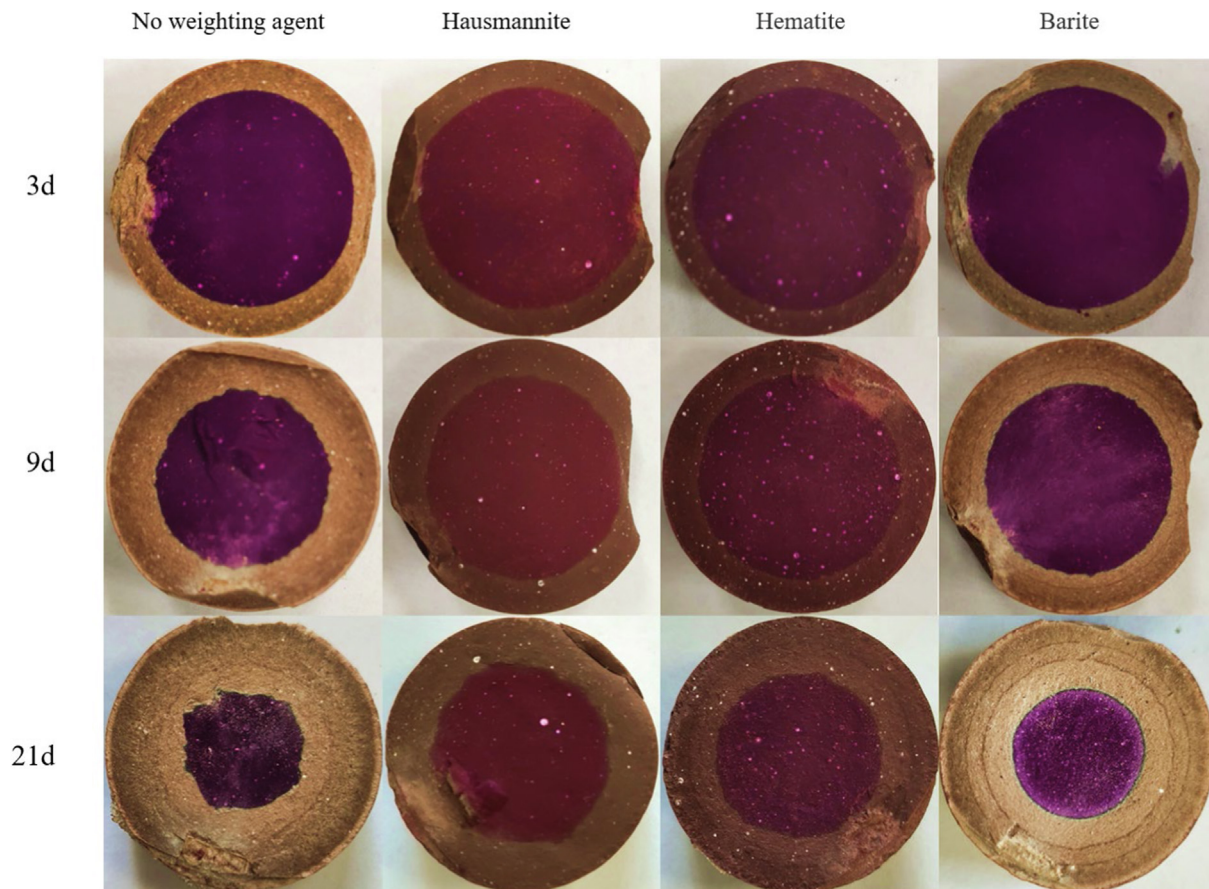


Fig. 5 Section diagrams of cement carbonation for 3, 9, and 21 days.

Table 4 Cement carbonation 21 days of carbonation data.

| Weighting agents | S ₁ (mm ²) | D (mm) | P (%) |
|--------------------|-----------------------------------|--------|-------|
| No weighting agent | 93.6 | 7.04 | 80.9 |
| Hausmannite | 208.1 | 4.36 | 57.6 |
| Hematite | 177.3 | 4.99 | 63.9 |
| Barite | 111.4 | 6.55 | 77.3 |

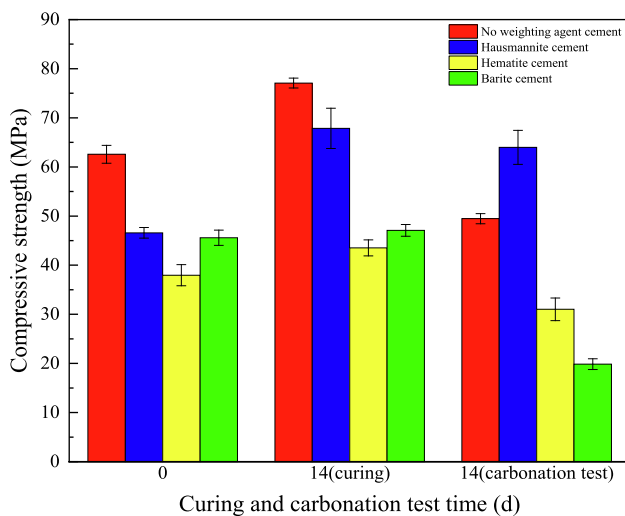
Table 5 Carbonation rate of cement in different periods.

| Weighting agents | v ₃ (mm/d) | v ₃₋₉ (mm/d) | v ₉₋₂₁ (mm/d) | v ₂₁ (mm/d) |
|--------------------|-----------------------|-------------------------|--------------------------|------------------------|
| No weighting agent | 0.91 | 0.30 | 0.21 | 0.34 |
| Hausmannite | 0.79 | 0.16 | 0.08 | 0.21 |
| Hematite | 0.78 | 0.13 | 0.16 | 0.24 |
| Barite | 0.81 | 0.25 | 0.22 | 0.31 |

stage, while the subsequent carbonation curing was unprofitable to the carbonation effect due to the generation of calcium carbonate prevents the diffusion of CO₂, making the subsequent carbonation become difficult (Wang et al., 2019). The overall trend of the carbonation rate of the cement was decreasing, except that the carbonation rate of hematite cement on the 9th to 12th day was slightly higher than that on the 3rd to the ninth day. In the carbonation time of 21 days, the carbonation rate of hausmannite cement was the lowest, and the carbonation rate of cement without weighting agents was the highest.

3.1.2. Effect of weighting agent on compressive strength after corrosion

Compressive strength is an essential property of oil well cement. Fig. 6 shows the influence of carbonation on the compressive strength of cement. The cement curing for three days was used as the base sample. Then the cement was divided into two batches, respectively, continuing for two weeks of curing (no CO₂) and carbonation test. With the continuous hydration reaction, the compressive strength of cement after two weeks of continuous curing was improved compared with the com-

**Fig. 6** Change of cement compressive strength.

pressive strength of the base samples. Among them, the compressive strength of hausmannite cement increased most significantly by 45.7 %; the compressive strength of hematite cement increased by 14.7 %; the compressive strength of barite cement increased the least and had no noticeable change. The further hydration of cement is the main reason for the increase in compressive strength of the cement set. The change of compressive strength reflects the early hydration rate of different cement sets. It can be known that the early hydration rate of hausmannite cement is slow, and the compressive strength is greatly improved with the extension of curing time. However, the early hydration rate of barite is faster, and the compressive strength is close to the peak after curing for three days. Hydration products of Portland cement are alkaline. When the hydration time is short, Portland cement has not generated many hydration products and CO₂ medium reactions (Costa et al., 2018). The faster hydration speed may be the reason for the faster carbonation rate of barite cement. After carbonation for two weeks, the compressive strength of cement decreased to different degrees compared with cement cured for the same time. The compressive strength of the hausmannite cement decreased the least, while that of the barite cement decreased significantly.

3.2. Effect of weighting agent on microstructure of corroded cement paste

3.2.1. X-ray diffraction analysis of cement sample

Fig. 7 shows that in the physical phase of cement, the unreacted SiO₂, the carbonized product CaCO₃, and the weighting material itself (Mn₃O₄, Fe₂O₃, and BaSO₄) had prominent characteristic peaks. Compared with the uncarbonized zone, the carbonized zone was rich in carbonized product CaCO₃, which mainly existed in the carbonized zone in three forms, namely calcite, aragonite, and vaterite. Calcite widely existed in all kinds of cement and is the main carbonation product, aragonite mainly existed in cement without a weighting agent (Fig. 7a), hausmannite cement (Fig. 7b), and hematite cement (Fig. 7c), vaterite mainly existed in barite cement (Fig. 7d). Aragonite formed by reaction under high-temperature conditions is converted to vaterite when the pH value in the cement matrix drops to a level conducive to vaterite formation (Bjorge et al., 2019). At the beginning of the carbonation reaction, the calcium carbonate content increases with the reaction time, but after a longer time, the calcium carbonate content will appear to decrease, which may be related to the leaching of carbonate (Ledesma et al., 2020; Bjorge et al., 2019; Zhang et al., 2018). The cement stone containing weighting agent is rich in many non-alkaline substances, coupled with the rapid carbonation rate of barite cement stone, carbonation reaction constantly consumes alkaline hydration products in the cement matrix. These factors may cause the barite cement carbonation zone to be rich in vaterite. The peak value of calcite in cement without a weighting agent decreased significantly after carbonation for nine days compared with 30 days, indicating that the bicarbonate reaction began to take place in large quantities. On the contrary, the peak value of barite cement calcite increased significantly, indicating that the carbonation reaction was still in large quantities, which further indicated that the carbonation products generated by barite cement could not effectively inhibit the carbonation rate cement.

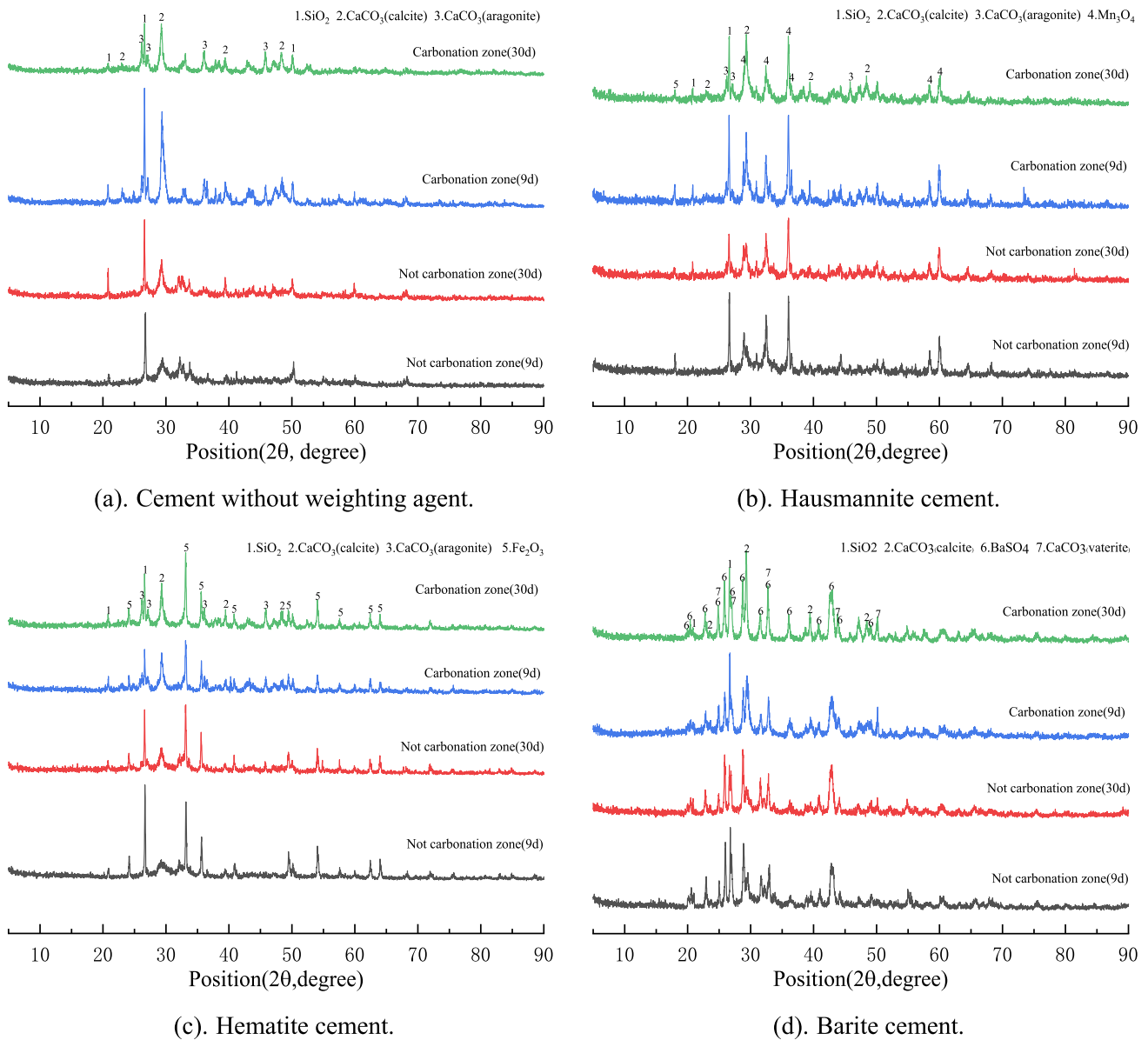


Fig. 7 XRD patterns of cement carbonation on the 9th and 30th day.

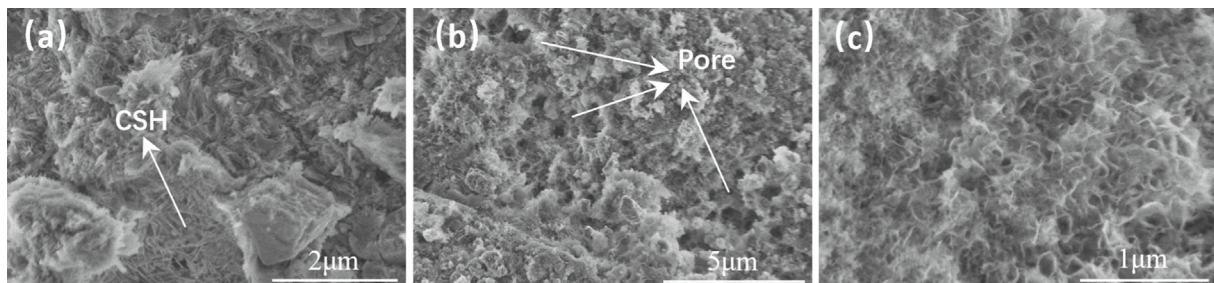


Fig. 8 Cement without weighting agent (a is in the uncarbonized zone, b and c are in the carbonized zone).

3.2.2. Scanning electron microscopy test of cement sample

The microstructure of cement before and after carbonation can be observed by scanning an electron microscope. Fig. 8, Fig. 9, Fig. 10, and Fig. 11 show SEM images of the uncar-

bonized zone and carbonized zone of cement set after 30 days of carbonation. The uncarbonized layer of cement was rich in calcium silicate hydrate (CSH), and the presence of CSH can provide strength for cement (Zhang et al., 2023). The carbon-

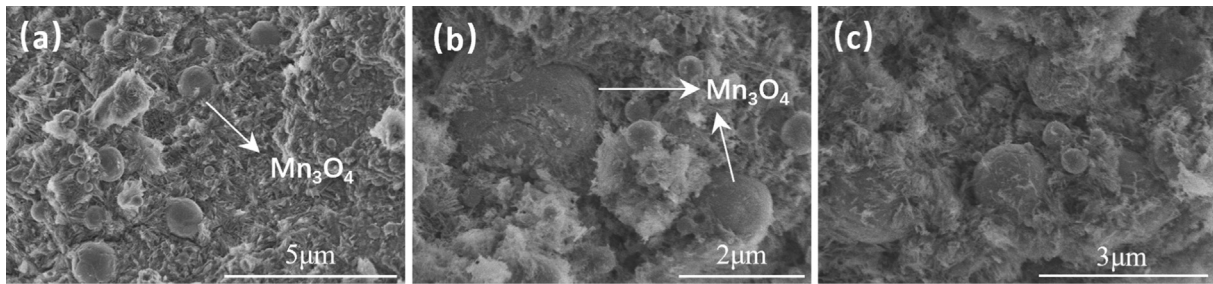


Fig. 9 Cement with Hausmannite (a is in the uncarbonized zone, b and c are in the carbonized zone).

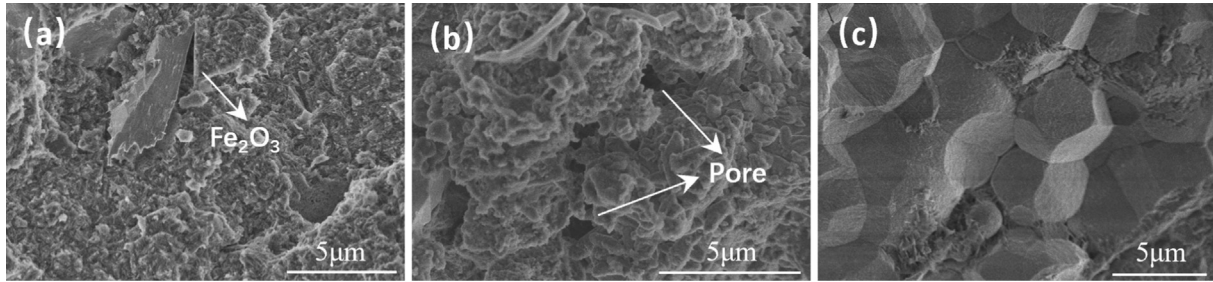


Fig. 10 Cement with Hematite (a is in the uncarbonized zone, b and c are in the carbonized zone).

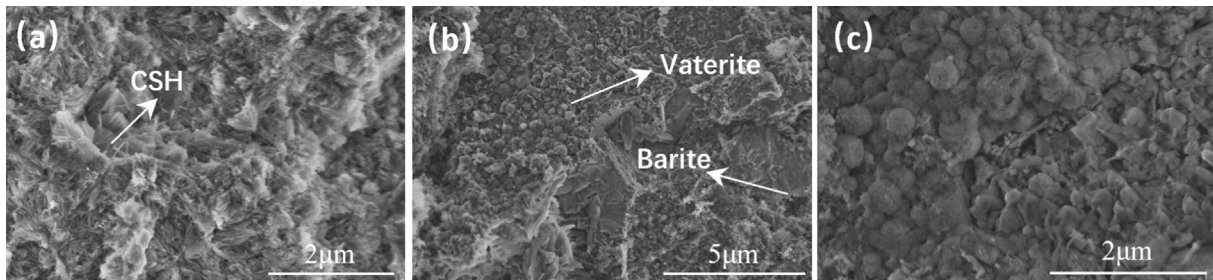


Fig. 11 Cement with Barite (a is in the uncarbonized zone, b and c are in the carbonized zone).

ation reaction consumes CSH, which is a process of volume shrinkage (Shen et al., 2016). Therefore, compared with CaCO_3 , CSH is more conducive to the densification of cement structures. Carbonation generated amorphous SiO_2 after CSH reaction, as shown in Fig. 8c. The cement carbonation zone structure was looser, with more pores. Unlike irregularly shaped hematite and barite, spherical Mn_3O_4 (Fig. 9) has a more vital mixing ability and is more evenly dispersed in cement. If the mineral materials are not evenly dispersed, it is easy to see the phenomenon of particle aggregation, as shown in Fig. 10c. A large amount of vaterite could be found in the barite cement carbonation zone (Fig. 11c), consistent with the conclusion in Fig. 7d. The formation of vaterite proved that the carbonization rate of barite cement was fast.

3.2.3. Pore diameter distribution of cement sample

The Mercury injection method is used to analyze the pore diameter distribution of cement after carbonation, and the influence of carbonation on the pore structure of cement can be learned. The pore diameter of cement paste falls into four categories: gel pores (diameter < 10 nm), transitional pores (diameter, 10 ~ 100 nm), capillary pores (diameter,

100 ~ 1000 nm) and macropores (diameter > 1000 nm) in light of the natural distribution of the pore structure. Pores larger than 50 nm in diameter can be regarded as harmful pores (Wang et al., 2020; Zhang et al., 2017). As can be seen from the pore size distribution of cement stones in Fig. 12, the pore diameter distribution of all cement stones is mainly concentrated within 100 nm. Unlike barite cement, the pore diameter distribution of other cement has a similar trend after carbonation. That is, the pore diameter of the most distributed pore becomes small. It is worth noting that although barite cement has a faster carbonation rate, the pores with the most extensive distribution of uncarbonized zones have the most minor pore diameters (Fig. 12d). It indicates that under initial conditions (without carbonation), more small pore size does not mean a slower carbonation rate.

Fig. 13 shows the volume distribution of different types of pores in different cement samples. Compared with cement without adding a weighting agent, the volume of uncarbonized zone pore of cement with a weighting agent was smaller. Adding weight agent can effectively reduce the porosity of cement stone (Ahmed et al., 2019). Compared with the uncarbonized zone, the pore volume of all cement increased significantly.

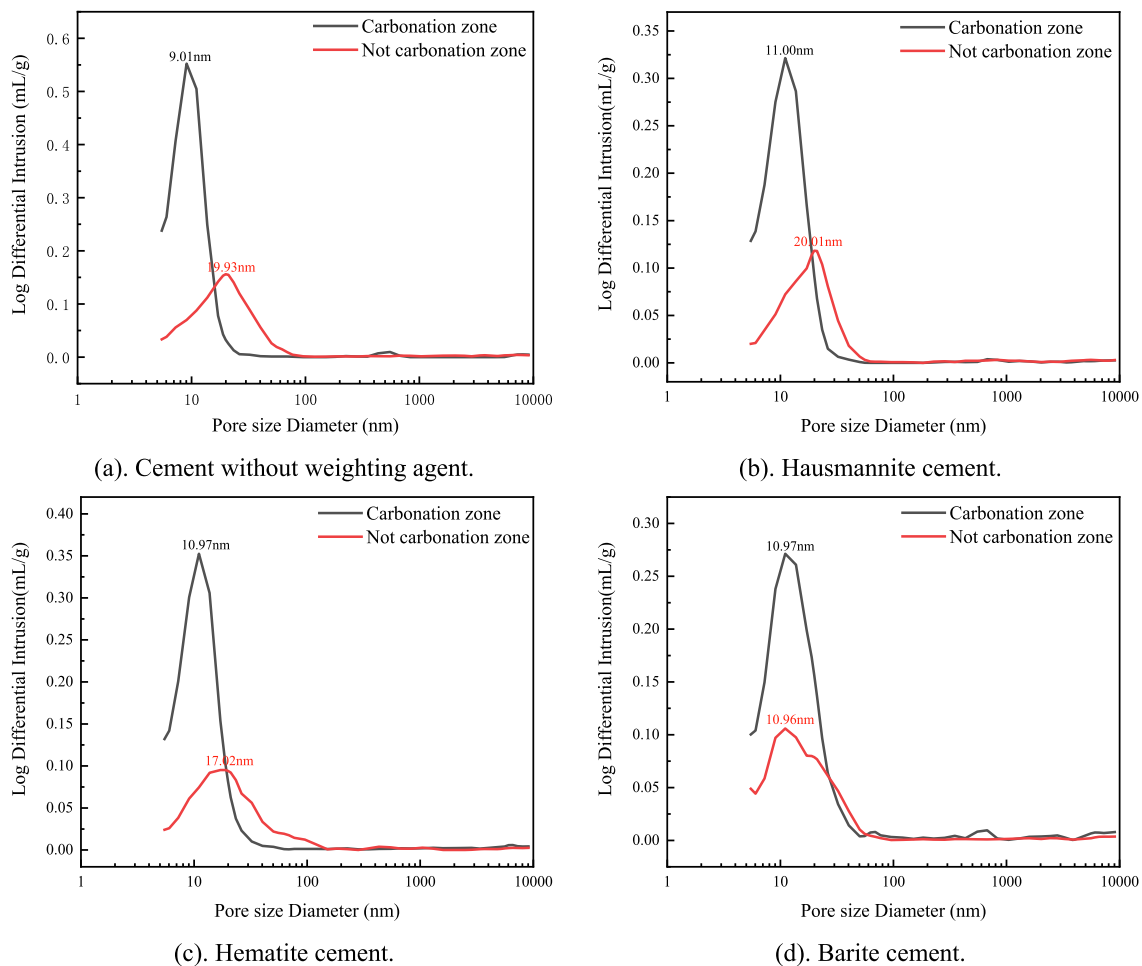


Fig. 12 Differential pore-size distributions of the specimens after carbonation for 30 days.

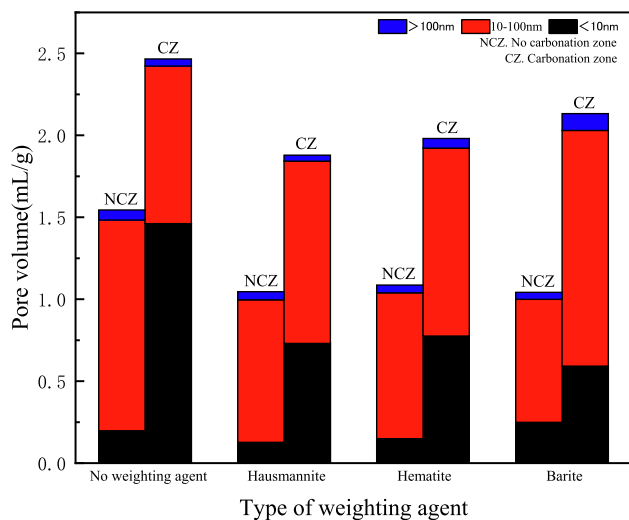


Fig. 13 Pore volume distribution after carbonation for 30 days.

The pore volume of cement without weighting agent increased by 59.6 %, that of hausmannite cement increased by 79.6 %, that of hematite cement increased by 82.3 %, and that of barite cement increased by 104.6 %. The pore volume of cement without a weighting agent had the slightest change; the pore

volume of the uncarbonized zone and the carbonation zone was the largest. The change of pore volume of hausmannite cement was the least in the cement with a weighting agent.

According to the proportions of different pores in not carbonation zones (NCZ) and carbonation zones (CZ) of the cement samples in Table 6, it can be seen that more than 95 % of the pore diameter of cement pore was less than 100 nm. There are a lot of pores in hardened oil well cement slurry. These are mainly composed of capillaries less than 10 nm in diameter and gel pores. The porosity with large diameter has a destructive effect on the strength of cement stone (Zhang et al., 2018; Wang et al., 2017). The pore diameter changes of different cement had similar rules. The pores with diameters smaller than 10 nm increased, and those with pore diameters between 10 nm and 100 nm decreased. The difference was that barite cement pores with pore diameter greater than 100 nm increased while other cement decreased. Of all types of cement, the proportion of pore volume with large pores size (diameter greater than 100 nm) of hausmannite cement decreased the most, which might be an important reason for its lowest carbonation rate. It is worth noting that although the proportion of the number of pores less than 10 nm in the uncarbonized zone of barite cement was the largest, the proportion of the number of pores less than 10 nm in the carbonation zone was the smallest. The rapid carbonation

Table 6 Percentage of pore size of different types of cement.

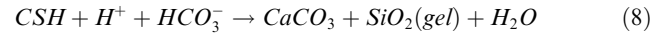
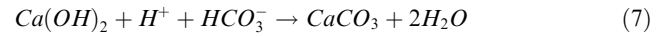
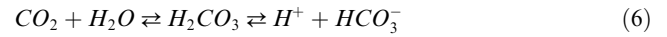
| Type of weighting agent | Different types of pore volume (%) | | | | | |
|-------------------------|------------------------------------|------|-----------|------|----------|-----|
| | < 10 nm | | 10–100 nm | | > 100 nm | |
| | NCZ | CZ | NCZ | CZ | NCZ | CZ |
| No weighting agent | 12.8 | 59.3 | 83.3 | 39.0 | 3.9 | 1.7 |
| Hausmannite | 12.1 | 38.9 | 83.1 | 59.2 | 4.8 | 1.9 |
| Hematite | 13.8 | 39.1 | 81.9 | 57.9 | 4.4 | 3.0 |
| Barite | 23.9 | 27.8 | 72.0 | 67.4 | 4.1 | 4.8 |

rate of cement without a weighting agent might be due to its sizeable initial pore volume. However, the poor ability of barite cement to generate tiny pores (pore diameter less than 10 nm) after carbonation may be the reason for its rapid carbonation rate.

3.3. Discussion on carbonation mechanism of cement sample

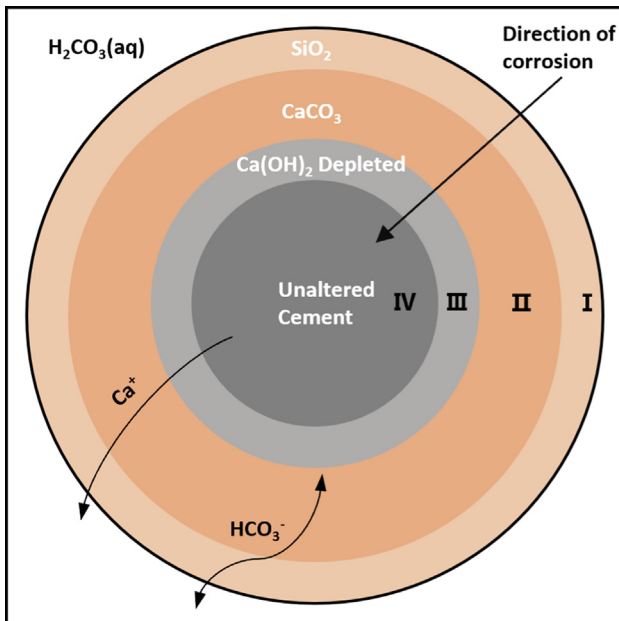
Commonly used oil well cement belongs to the Portland cement series, silicate mineral mass fraction accounts for about 80 %, its main mineral composition is C_3S and C_2S (Mei et al., 2020). The hydration reaction occurs, and corresponding hydration products are generated (Eq.5) when various cement components are in contact with water. Currently, it is generally accepted that the reaction process of cement carbonization is divided into four regions with cement as the matrix (Kutchko et al., 2007; Mason et al., 2013), as shown in Fig. 14. Cement is in an acidic environment rich in carbonic acid (Eq.6). The outermost region is the area rich in silica, in which the hydration products and carbonation products are consumed, and amorphous SiO_2 remains. Eq. (9) reacts at the interface of II and I, and the generated bicarbonate ion is transported outward. At the same time, the generated $Ca(HCO_3)_2$ will further consume Ca^{+} , resulting in reaction Eq.

(10), which promotes the carbonation reaction. II is the undissolved calcium carbonate zone, and III is the $Ca(OH)_2$ depletion zone. In region 3, under the action of concentration difference, hydration product $Ca(OH)_2$ dissolves preferentially, Ca^{+} migrates outward, and a carbonation reaction occurs (Eq. (7)). $Ca(OH)_2$ is consumed, and CSH that has not participated in the carbonation reaction remains. Region 2 continues to develop internally, further consuming CSH and producing a reaction (Eq.8). IV is the unreacted zone, in which the physical and chemical properties of cement have not changed.



The carbonation of cement is a complex process, and the carbonization of oil well cement is also affected by many factors. The carbonation mechanism may differ under different conditions. In the carbonation process of high-temperature sand cement, due to the addition of many siliceous materials, cement hydration products at high temperatures do not contain $Ca(OH)_2$. Therefore, there is no $Ca(OH)_2$ dissolution process (Costa and d. S., Freitas, J. C. d. O., Santos, P. H. S., Melo, D. M. d. A., Araujo, R. G. d. S., Oliveira, Y. H. d., , 2018; Jiang et al., 2021). Therefore, the carbonation front of cement with silica sand may be different from that without silica sand (Björge et al., 2019). In this paper, the admixture of cement slurry has many weighting materials besides silica sand. Although the weighting material only plays the role of filling and weighting and does not participate in cement's hydration and carbonation reaction, different weighting agents have different effects on the carbonation of cement.

When adding a large number of foreign admixtures that do not participate in the reaction, the carbonization rate of cement needs to consider the influence of foreign admixtures on the cement hydration rate (Briki et al., 2021). In laboratory tests, cement is often chosen to be cured for 3–7 days before carbonation reaction, but in fact, cement slurry begins to solidify when it is injected underground. At the same time, it is also necessary to consider whether cement carbonization can form a more dense carbonation zone. There may be many factors affecting the formation of dense carbonation zone after the

**Fig. 14** Reaction process of CO_2 corroding cement.

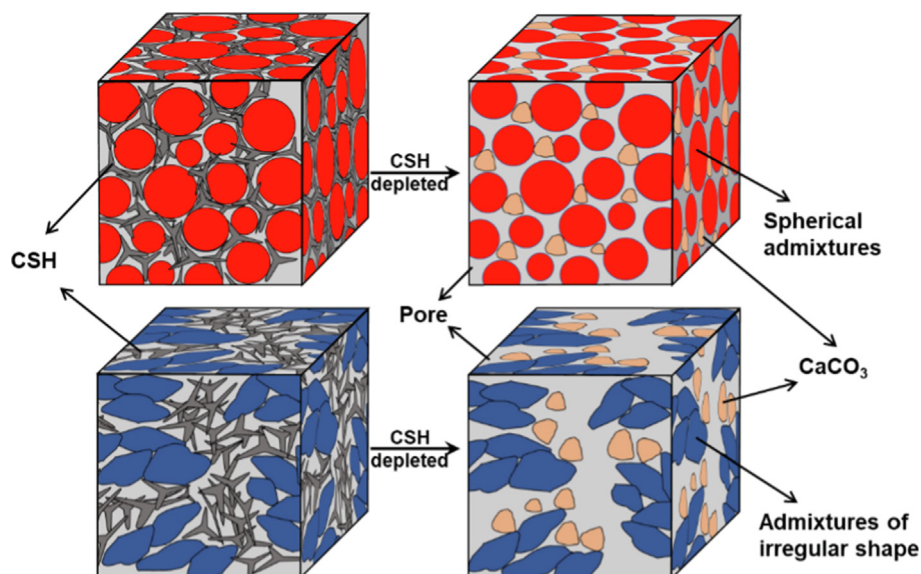


Fig. 15 Schematic diagram of pore structure change after carbonation of cement with different fillers.

carbonation of cement. In comparing the carbonation rate of cement without a weighting agent and cement with a weighting agent, the water–solid ratio is the main factor (Mu et al., 2017). Because the weighting agent increases the density of cement slurry and plays a role in filling pores, under the same water consumption condition, the pore volume of three kinds of cement with weighting agents is smaller than that without a weighting agent. Secondly, the influence of pore volume of the cement carbide layer may also be related to the dispersion degree of weighting agent particles in the cement slurry system. As shown in Fig. 15, hausmannite particles are more evenly distributed in the cement slurry system because of their spherical shape, which better mixing ability than the irregularly shaped weighting agent. As weighting agent itself does not participate in the carbonation reaction but mainly plays a filling role. Therefore, when the carbonation reaction consumes CSH, the spherical weighting agent with more uniform dispersion forms relatively small pores. Smaller pores are also more likely to retain CaCO_3 generated by carbonization, thus reducing the formation of large pores.

4. Conclusion

According to the experimental results, the following are conclusions in this study.

- (1) Different weighting agents have different effects on the hydration rate of cement. Barite cement stone hydration rate is the fastest, hausmannite cement stone hydration rate is the slowest. Although the rapid hydration rate is beneficial to the development of compressive strength, it will harm the carbonation of cement.
- (2) Cement carbide mainly exists in three forms, namely, calcite, aragonite, and vaterite. Among them, calcite is the main carbonation product of all cement, and vaterite mainly exists in the carbonation zone of barite cement, while it is more contained in the carbonation zone of hausmannite cement and hematite cement. The mass production of vaterite is the manifestation of the high carbonation rate of barite cement.

- (3) In the process of carbonation, the pore structure of cement is mainly reflected in the increase of the number of pores with pores diameter less than 10 nm, and the proportion of the number of pores with pores diameter greater than 100 nm decreases. The pore size larger than 100 nm occupies the least proportion in hausmannite cement and the highest proportion in barite cement. The formation of tiny pores whose diameters are less than 10 nm is an important reason to reduce the carbonation rate. The pore structure changes are different after the carbonation of cement with different weighting agents. The cement with a more dense carbonation zone has a slower carbonation rate. Among the three weighting agents (hausmannite, hematite, and barite), hausmannite has the best effect on slowing down the carbonation rate of cement.

Declaration of Competing Interest

The authors declare that they have no known competing financial interests or personal relationships that could have appeared to influence the work reported in this paper.

Acknowledgment

The author would like to acknowledge the project supported by the Open Fund (UOG2022-24) of Cooperative Innovation Center of Unconventional Oil and Gas (Ministry of Education & Hubei Province), Yangtze University (Ministry of Education & Hubei Province).

References

- Abdel-Basset, M., Al-Otaibi, Y., Al-Saeed, A., Blushi, T., Fidan, E., Al-Mutawa, M., Abdelbagi, M., Hadi, A., 2021. In Paradigm shift from cemented completions to multi-stage completion strategy for managing tight gas development challenges. Abu Dhabi Int. Petroleum Exhibition Conf., OnePetro. <https://doi.org/10.2118/207705-MS>.
- Abed, A., El Gohary, M., Snaineh, A., Guettat, M., Ahmad, M., Lozano, J., Al Reyami, M., 2010. In Deep Sour Gas Reservoir

- Development and Challenges. SPE Deep Gas Conf. Exhibition, OnePetro. <https://doi.org/10.2118/130899-MS>.
- Ahmed, A., Mahmoud, A.A., Elkhatny, S., Chen, W., 2019. The effect of weighting materials on oil-well cement properties while drilling deep wells. *Sustainability* 11 (23), 6776. <https://doi.org/10.3390/su11236776>.
- Allen, D., Strazisar, B., Soong, Y., Hedges, S., 2005. Modeling carbon dioxide sequestration in saline aquifers: significance of elevated pressures and salinities. *Fuel Process. Technol.* 86 (14–15), 1569–1580. <https://doi.org/10.1016/j.fuproc.2005.01.004>.
- Bachu, S., 2000. Sequestration of CO₂ in geological media: criteria and approach for site selection in response to climate change. *Energy Convers. Manage.* 41 (9), 953–970. [https://doi.org/10.1016/S0196-8904\(99\)00149-1](https://doi.org/10.1016/S0196-8904(99)00149-1).
- Bagheri, M., Shariatipour, S.M., Ganjian, E., 2018. A review of oil well cement alteration in CO₂-rich environments. *Constr. Build. Mater.* 186, 946–968. <https://doi.org/10.1016/j.conbuildmat.2018.07.250>.
- Batista, G.d.S., Schemmer, L.B., Siqueira, T.d.A., Costa, E.M.d., 2021. Chemical resistance and mechanical properties of nano silica addition in oil well cement. *J. Petroleum Sci. Eng.* 196, 107742. <https://doi.org/10.1016/j.petrol.2020.107742>.
- Bjorge, R., Gawel, K., Panduro, E.A.C., Torsæter, M., 2019. Carbonation of silica cement at high-temperature well conditions. *Int. J. Greenhouse Gas Control* 82, 261–268. <https://doi.org/10.1016/j.ijggc.2019.01.011>.
- Briki, Y., Zajac, M., Haha, M.B., Scrivener, K., 2021. Impact of limestone fineness on cement hydration at early age. *Cem. Concr. Res.* 147, <https://doi.org/10.1016/j.cemconres.2021.106515> 106515.
- Bruckdorfer, R.A., 1986. In Carbon Dioxide Corrosion in Oilwell Cements. SPE Rocky Mountain Regional Meeting. <https://doi.org/10.2118/15176-MS>.
- Caritey, J.-P., Brady, J., 2013. In Performance of thermal cements with different weighting materials, SPE/IADC Drilling Conference, OnePetro. <https://doi.org/10.2118/163544-MS>.
- Contreras, E.Q., Santra, A., 2021. In Wellbore Integrity and CO₂ Sequestration Using Polyaramide Vesicles. SPE Int. Conf. Oilfield Chem. <https://doi.org/10.2118/204385-MS>.
- Costa, B.L.d.S., Freitas, J.C.d.O., Santos, P.H.S., Melo, D.M.d.A., Araujo, R.G.d.S., Oliveira, Y.H.d., 2018. Carbonation in oil well Portland cement: Influence of hydration time prior to contact with CO₂. *Construct. Build. Mater.* 159, 252–260. <https://doi.org/10.1016/j.conbuildmat.2017.10.103>.
- Costa, B.L.S., Freitas, J.C.O., Araujo, R.G.S., Oliveira, Y.H., Santiago, R.C., Oliveira, F.S., 2021. Analysis of different oil well cement slurry formulations exposed to a CO₂-rich environment. *J. CO₂ Utilization* 51, <https://doi.org/10.1016/j.jcou.2021.101636> 101636.
- Drouet, E., Poyet, S., Le Bescop, P., Torrenti, J.-M., Bourbon, X., 2019. Carbonation of hardened cement pastes: influence of temperature. *Cem. Concr. Res.* 115, 445–459. <https://doi.org/10.1016/j.cemconres.2018.09.019>.
- Elkhatny, S., 2021. Improved carbonation resistance and durability of Saudi Class G oil well cement sheath in CO₂ rich environments using laponite. *J. Pet. Sci. Eng.* 196, <https://doi.org/10.1016/j.petrol.2020.107812> 107812.
- Engelke, B., de Miranda, C.R., Daou, F., Petersen, D., Aponte, S.A., Oliveira, F., Ocando, L.M., Conceição, A. C., Guillot, D., 2017. In: CO₂ Self-Healing and Resistant Cement Technology From Laboratory to the Field, SPE/IADC Drilling Conference, and Exhibition. <https://doi.org/10.2118/184641-MS>.
- Fakhr Eldin, Y., Irvine-Fortescue, J., Grieve, J., Taoutaou, S., Jain, B., Al Kalbani, S., Thery, F., 2009. In The use of specialized cement to ensure long term zonal isolation for sour wells in south Oman. *Int. Petroleum Technol. Conf. OnePetro.* <https://doi.org/10.2523/IPTC-13400-MS>.
- Guang, Y., Zhanyin, Z., Mingli, S., 2011. Formation of carbon dioxide and hydrocarbon gas reservoirs in the Changling fault depression, Songliao Basin. *Petroleum Exploration Dev.* 38 (1), 52–58. [https://doi.org/10.1016/s1876-3804\(11\)60014-1](https://doi.org/10.1016/s1876-3804(11)60014-1).
- Hoa, L.Q., Bäßler, R., Bettge, D., Buggisch, E., Schiller, B.N., Beck, M., 2021. Corrosion study on wellbore materials for the CO₂ injection process. *Processes* 9 (1), 115. <https://doi.org/10.3390/pr9010115>.
- Jani, P., Imqam, A., 2021. Class C fly ash-based alkali-activated cement as a potential alternative cement for CO₂ storage applications. *J. Pet. Sci. Eng.* 201, <https://doi.org/10.1016/j.petrol.2021.108408> 108408.
- Jiang, T., Geng, C., Yao, X., Song, W., Dai, D., Yang, T., 2021. Long-term thermal performance of oil well cement modified by silica flour with different particle sizes in HTHP environment. *Constr. Build. Mater.* 296, <https://doi.org/10.1016/j.conbuildmat.2021.123701> 123701.
- Jihai, Y., Huang, B., 2019. Origin and migration model of natural gas in L gas field, eastern slope of Yinggehai Sag, China. *Pet. Explor. Dev.* 46 (3), 471–481. [https://doi.org/10.1016/s1876-3804\(19\)60028-5](https://doi.org/10.1016/s1876-3804(19)60028-5).
- Kiran, R., Teodoriu, C., Dadmohammadi, Y., Nygaard, R., Wood, D., Mokhtari, M., Salehi, S., 2017. Identification and evaluation of well integrity and causes of failure of well integrity barriers (A review). *J. Nat. Gas Sci. Eng.* 45, 511–526. <https://doi.org/10.1016/j.jngse.2017.05.009>.
- Krilov, Z., Loncaric, B., Miksa, Z., 2000. Investigation of a long-term cement deterioration under a high-temperature, sour gas downhole environment. SPE Int. Symposium Formation Damage Control. <https://doi.org/10.2118/58771-MS>.
- Kutchko, B.G., Strazisar, B.R., Dzombak, D.A., Lowry, G.V., Thaulow, N., 2007. Degradation of well cement by CO₂ under geologic sequestration conditions. *Environ. Sci. Tech.* 41 (13), 4787–4792. <https://doi.org/10.1021/es062828c>.
- Ledesma, R.B., Lopes, N.F., Bacca, K.G., Moraes, M.K.d., Batista, G.d.S., Pires, M.R., Costa, E.M.d., 2020. Zeolite and fly ash in the composition of oil well cement: Evaluation of degradation by CO₂ under geological storage condition. *J. Petroleum Sci. Eng.* 185, <https://doi.org/10.1016/j.petrol.2019.106656>.
- Lesti, M., Tiemeyer, C., Plank, J., 2013. CO₂ stability of Portland cement-based well-cementing systems for use on carbon capture & storage (CCS) wells. *Cem. Concr. Res.* 45, 45–54. <https://doi.org/10.1016/j.cemconres.2012.12.001>.
- Lu, Y., Liu, R., Wang, K., Tang, Y., Cao, Y., 2021. A study on the fuzzy evaluation system of carbon dioxide flooding technology. *Energy Sci. Eng.* 9 (2), 239–255. <https://doi.org/10.1002/ese3.844>.
- Mahmoud, A.A., Elkhatny, S., 2020. Improving class G cement carbonation resistance for applications of geologic carbon sequestration using synthetic polypropylene fiber. *J. Nat. Gas Sci. Eng.* 76, <https://doi.org/10.1016/j.jngse.2020.103184> 103184.
- Mason, H.E., Du Frane, W.L., Walsh, S.D.C., Dai, Z., Charnvanichborikarn, S., Carroll, S.A., 2013. Chemical and mechanical properties of wellbore cement altered by CO₂-rich brine using a multianalytical approach. *Environ. Sci. Tech.* 47 (3), 1745–1752. <https://doi.org/10.1021/es3039906>.
- Mei, K., Cheng, X., Pu, Y., Ma, Y., Gao, X., Yu, Y., Zhang, C., Zhuang, J., Guo, X., 2020. Evolution of silicate structure during corrosion of tricalcium silicate (C3S) and dicalcium silicate (C2S) with hydrogen sulphide (H₂S). *Corros. Sci.* 163, <https://doi.org/10.1016/j.corsci.2019.108301> 108301.
- Mei, K., Zhang, L., Wang, Y., Cheng, X., Xue, Q., Gan, M., Fu, X., Zhang, C., Li, X., 2022. Structural evolution in micro-calcite bearing Ca-montmorillonite reinforced oilwell cement during CO₂ invasion. *Constr. Build. Mater.* 315, <https://doi.org/10.1016/j.conbuildmat.2021.125744> 125744.
- Mi, R., Pan, G., Li, Y., Kuang, T., 2021. Carbonation degree evaluation of recycled aggregate concrete using carbonation zone widths. *J. CO₂ Util.* 43, <https://doi.org/10.1016/j.jcou.2020.101366> 101366.
- Mu, S., Liu, J., Lin, W., Wang, Y., Liu, J., Shi, L., Jiang, Q., 2017. Property and microstructure of aluminosilicate inorganic coating

- for concrete: Role of water to solid ratio. *Constr. Build. Mater.* 148, 846–856. <https://doi.org/10.1016/j.conbuildmat.2017.05.070>.
- Nianyin, L., Jiajie, Y., Chao, W., Suiwang, Z., Xiangke, L., Jia, K., Yuan, W., Yinong, D., 2021. Fracturing technology with carbon dioxide: A review. *J. Pet. Sci. Eng.* 205, <https://doi.org/10.1016/j.petrol.2021.108793> 108793.
- Omosebi, O., Maheshwari, H., Ahmed, R., Shah, S., Osisanya, S., Santra, A., Saasen, A., 2015. Investigating temperature effect on degradation of well cement in HPHT carbonic acid environment. *J. Nat. Gas Sci. Eng.* 26, 1344–1362. <https://doi.org/10.1016/j.jngse.2015.08.018>.
- Ponzi, G.G.D., Santos, V.H.J.M.d., Martel, R.B., Pontin, D., Stepanha, A.S.D.G.E., Schütz, M.K., Menezes, S.C., Einloft, S.M.O., Vecchia, F.D., 2021. Basalt powder as supplementary cementitious material in cement paste for CCS wells: chemical and mechanical resistance of cement formulations for CO₂ geological storage sites. *Int. J. Greenhouse Gas Control* 109, 103337. <https://doi.org/10.1016/j.ijggc.2021.103337>.
- Ramazanov, Y., Akhmetzianov, I., Sukhachev, V., Sozonov, A., Nafikova, S., Yuldashev, S., Jain, B., Zvyagin, V., Kim, A. and Khamidullin, D., 2021. Heavy Weight Cement System for Corrosive Environment: Preventing Strength Retrogression and H₂S Corrosion. In: SPE Annual Caspian Technical Conference, OnePetro. <https://doi.org/10.2118/207016-MS>.
- Ridha, S., Dzulkarnain, I., Abdurrahman, M., Ilyas, S.U., Bataee, M., 2021. Microstructural properties and compressive strength of fly ash-based geopolymer cement immersed in CO₂-saturated brine at elevated temperatures. *Int. J. Environ. Sci. Technol.* <https://doi.org/10.1007/s13762-021-03665-9>.
- Sedić, K., Ukrainczyk, N., Mandić, V., Gaurina-Međimurec, N., Šipušić, J., 2020. Carbonation of Portland-Zeolite and geopolymer well-cement composites under geologic CO₂ sequestration conditions. *Cem. Concr. Compos.* 111, <https://doi.org/10.1016/j.cemconcomp.2020.103615> 103615.
- Shah, P.H., Pandya, H.T., Sharma, H., Saxena, A., 2012. Offshore drilling & well testing of a HPHT gas well: a case study. SPE Oil and Gas India Conference and Exhibition, OnePetro. <https://doi.org/10.2118/155320-MS>.
- Shen, Q., Pan, G., Bao, B., 2016. Influence of CSH carbonation on the porosity of cement paste. *Mag. Concr. Res.* 68 (10), 504–514. <https://doi.org/10.1680/jmacr.15.00286>.
- Shiming, Z., Gensheng, L., Qichun, W., 2013. Research and preparation of ultra-heavy slurry. *Pet. Explor. Dev.* 40 (1), 115–118. [https://doi.org/10.1016/s1876-3804\(13\)60012-9](https://doi.org/10.1016/s1876-3804(13)60012-9).
- Shujie, L., Zhong, L., Jin, Y., Renjun, X., Yanjun, L., Gang, T., Ming, L., Yi, W., Guoxian, X., Qishuai, Y., 2020. Key Technology and Industrial Application of HPHT Drilling and Completion in the South China Sea. Offshore Technology Conference, OnePetro. <https://doi.org/10.4043/30594-MS>.
- Srivastava, A., Ahmed, R., Shah, S., 2019. Carbonic acid resistance of hydroxyapatite based cement. SPE Int. Conf. Oilfield Chem. <https://doi.org/10.2118/193585-MS>.
- Teodoriu, C., Bello, O., 2020. A review of cement testing apparatus and methods under CO₂ environment and their impact on well integrity prediction—Where do we stand? *J. Pet. Sci. Eng.* 187, <https://doi.org/10.1016/j.petrol.2019.106736> 106736.
- Tiong, M., Gholami, R., Abid, K., Ekhlaur Rahman, M., 2020. Nanomodification: an efficient method to improve cement integrity in CO₂ storage sites. *J. Nat. Gas Sci. Eng.* 84, <https://doi.org/10.1016/j.jngse.2020.103612> 103612.
- Vishal, V., Chandra, D., Singh, U., Verma, Y., 2021. Understanding initial opportunities and key challenges for CCUS deployment in India at scale. *Resour. Conserv. Recycl.* 175, <https://doi.org/10.1016/j.resconrec.2021.105829> 105829.
- Wang, Y., Yuan, Q., Deng, D., Liu, Z., 2017. Modeling compressive strength of cement asphalt composite based on pore size distribution. *Constr. Build. Mater.* 150, 714–722. <https://doi.org/10.1016/j.conbuildmat.2017.06.049>.
- Wang, Y., Lang, X., Fan, S., Wang, S., Yu, C., Li, G., 2021. Review on Enhanced Technology of Natural Gas Hydrate Recovery by Carbon Dioxide Replacement. *Energy Fuel* 35 (5), 3659–3674. <https://doi.org/10.1021/acs.energyfuels.0c04138>.
- Wang, S.Y., McCaslin, E., White, C.E., 2020. Effects of magnesium content and carbonation on the multiscale pore structure of alkali-activated slags. *Cem. Concr. Res.* 130, <https://doi.org/10.1016/j.cemconres.2020.105979> 105979.
- Wang, J.B., Xu, H.X., Xu, D.Y., Du, P., Zhou, Z.H., Yuan, L.W., Cheng, X., 2019. Accelerated carbonation of hardened cement pastes: Influence of porosity. *Construct. Build. Mater.* 225, 159–169. <https://doi.org/10.1016/j.conbuildmat.2019.07.088>.
- Wei, P., Juan, D., Tongyi, Z., Zhiguo, Q., Gang, L., 2015. Well Testing Technique for HPHT Sour Gas Wells in China. Offshore Technology Conference, OnePetro. <https://doi.org/10.4043/25681-MS>.
- Xin, H., Zeng, J., Deng, Q., Wang, J., Shi, L., Zou, J., 2020. A Novel Calcium Phosphate Cement with Good CO₂ and H₂S Corrosion Resistance. In: The 30th International Ocean and Polar Engineering Conference.
- Xu, B., Yuan, B., Wang, Y., Zeng, S., Yang, Y., 2019. Nanosilica-latex reduction carbonation-induced degradation in the cement of CO₂ geological storage wells. *J. Nat. Gas Sci. Eng.* 65, 237–247. <https://doi.org/10.1016/j.jngse.2019.03.013>.
- Yang, Y., Yuan, B., Wang, Y., Zhang, S., Zhu, L., 2016. Carbonation resistance cement for CO₂ storage and injection wells. *J. Pet. Sci. Eng.* 146, 883–889. <https://doi.org/10.1016/j.petrol.2016.08.006>.
- Zhang, C., Song, Y., Wang, W., Guo, X., Li, H., 2017. The influence of sulfonated asphalt on the mechanical properties and microstructure of oil well cement paste. *Constr. Build. Mater.* 132, 438–445. <https://doi.org/10.1016/j.conbuildmat.2016.12.014>.
- Zhang, C., Li, Y., Cheng, X., Liang, S., Guo, X., Zhao, H., Song, Y., 2018. Effects of plasma-treated rock asphalt on the mechanical properties and microstructure of oil-well cement. *Constr. Build. Mater.* 186, 163–173. <https://doi.org/10.1016/j.conbuildmat.2018.07.133>.
- Zhang, J., Peng, Z., Zou, C., Chen, D., 2018. Improving the carbonation resistance of cement stone for oil wells by a polymer with acid response characteristic. *J. Pet. Sci. Eng.* 164, 382–389. <https://doi.org/10.1016/j.petrol.2018.01.080>.
- Zhang, Y., Wang, C., Chen, Z., Yu, Y., Jing, J., Xia, X., Liu, H., Meng, R., 2023. Research on the strength retrogression and mechanism of oil well cement at high temperature (240 °C). *Constr. Build. Mater.* 363, <https://doi.org/10.1016/j.conbuildmat.2022.129806> 129806.